

ULTIMATE STRENGTH EQUATION FOR PULTRUDED CFRP PLATES IN FIRE

Ke WANG

Engineer
AECOM Asia Co. Ltd
Transportation, AECOM, 138 Shatin Rural Committee Road, Hong Kong
wangrichard2011@gmail.com

Ben YOUNG

Professor
The University of Hong Kong
Department of Civil Engineering, The University of Hong Kong, Pokfulam, Hong Kong
young@hku.hk *

Scott T. SMITH

Associate Professor
The University of Hong Kong
Department of Civil Engineering, The University of Hong Kong, Pokfulam, Hong Kong
stsmith@hku.hk

Abstract

The paper presents a model for the ultimate strength calculation of fibre-reinforced polymer (FRP) pultruded plates in fire. The model is calibrated from a series of coupon tests on pultruded CFRP plates carried out using steady state and transient state test methods. In the steady state tests, temperatures ranging from ambient to approximately 700°C were considered. The test specimens were heated to a specified temperature then loaded until failure while the same temperature was maintained throughout the test. Different periods of times of 5 and 30 minutes were maintained to investigate the effect of heating duration. In the transient state tests, the test specimens were loaded to a specified stress level prior to heating, and then the temperature was increased until failure of the test specimens. Three different stress levels applied to the pultruded CFRP plates were considered. Based on the test results, an ultimate strength equation is proposed which has been inspired from a model developed for metallic materials subjected to elevated temperatures. Application of the model is finally demonstrated in a worked example.

Keywords: Elevated temperatures; Fire resistance; Pultruded CFRP plate; Ultimate strength equation.

1. Introduction

There are now many studies investigating the strengthening of reinforced concrete (RC) structural members with fibre-reinforced polymer (FRP) composites at room temperature or common operating temperatures [e.g. 1]. Characterisation of FRP materials and FRP-strengthened RC structures subjected to elevated temperatures and fire conditions are more limited though. Carbon and glass fibres, which are most commonly used for strengthening applications, can withstand very high temperature and in the case of carbon fibres this temperature can exceed 2000°C [1]. Epoxy resin, which is used in the resin matrix and to also bond the FRP composite to concrete surfaces, however, degrades mechanically with increased temperature. This degradation starts before the glass transition temperature, T_g , is reached. As a result, the ability of the resin matrix to transfer forces amongst the fibres is lost as well as the ability of the resin to transfer forces between externally bonded FRP strengthening to the bonded concrete [2]. The T_g can typically be

found to lie in the range of 50 to 90°C for commercially available products used in civil infrastructure applications [3] that are applied at ambient temperatures. Some research has been conducted though on the mechanical properties of FRP bar and plate products under elevated temperatures [e.g. 3]. More specifically, tensile coupon tests have been conducted as well as single-shear FRP-to-FRP bond tests, direct tension (pull-off) FRP-to-concrete bond tests and FRP-to-concrete double-shear shear bond tests after exposure to temperatures of up to 400°C. In all tests cases, the strengths were found to decrease at different rates as the temperatures increased. The tests conducted by Foster and Bisby [3] concentrated on the post fire behaviour. Other researchers [4, 5] have investigated the behaviour of FRP composite materials for temperatures up to 200°C. Furthermore, Cao et al. [6] investigated experimentally the tensile properties of CFRP and hybrid FRP sheets subjected to elevated temperatures, ranging from 16 to 200°C, and the strengths were found to reduce by up to 40 %. In general, information on the high temperature and residual properties of FRP composites used in civil applications is still quite scarce though, especially for pultruded FRP products for strengthening applications. Investigation of reinforced concrete, steel, stainless steel, and concrete encased steel composite structures at elevated temperatures have been conducted [e.g. 7-10] and such test approaches can be used to inform the testing of FRP pultruded plates at elevated temperatures.

The purpose of the study reported in this paper is to present a model for the calculation of the ultimate strength of pultruded carbon FRP (CFRP but herein in *FRP*) plates subjected to elevated temperatures ranging from room temperature (approximately 22°C) up to high temperatures which may be expected in a fire (i.e. up to about 700°C in this study). The model is informed from tests on flat coupon specimens prepared from commercially available pultruded FRP plates and then tested to failure in tension in a universal testing machine while under the influence of various steady state or transient temperature histories. In the steady state tests, the test specimens were heated to a specified temperature and then the tensile test carried out. In the transient tests, the specimens were loaded to a certain stress level and then the temperature was increased until the test specimens failed. The transient state tests are considered more realistic in a fire, however, for completeness, both steady state and transient state tests were conducted. In this paper, the coupon tests are initially described, followed by the ultimate strength model and finally application of the model in a worked example.

2. Experimental Investigation

2.1 Testing process

The tensile coupon testing was conducted in an MTS 810 universal testing machine and the temperature was applied by a high temperature MTS 653 furnace which was controlled by an MTS 409.83 temperature controller. The test set-up is shown in Figure 1 and the FRP specimen, furnace and temperature controller are evident. The furnace, which can reach temperatures as high as 1400°C, gained its heat from six pairs of silicon carbide heating elements which were arranged in three zones. These three zones were separated by insulation plates in order to facilitate uniform heating and better temperature control. This type of furnace is well suited when very low thermal gradient along the length of the test specimen are desired, which can be the case for tensile or fatigue tests.

A total of 34 test coupon specimens were prepared and tested to failure. The specimens were divided into 3 groups (G1-G3) as shown in Table 1. The first two groups (G1 and G2) corresponded to steady state tests. Group G1 had a holding time of 5 minutes while Group G2

had a longer holding time of 30 minutes. Group G3 consisted of the transient state tests. Sika CarboDur 1214 Pultruded Plates were used in this study for all coupon tests. The test coupons were cut to size in the laboratory in accordance with ACI 440.3R-04 [11] and complete details of the test setup and the test specimens are reported in Wang et al. [12].

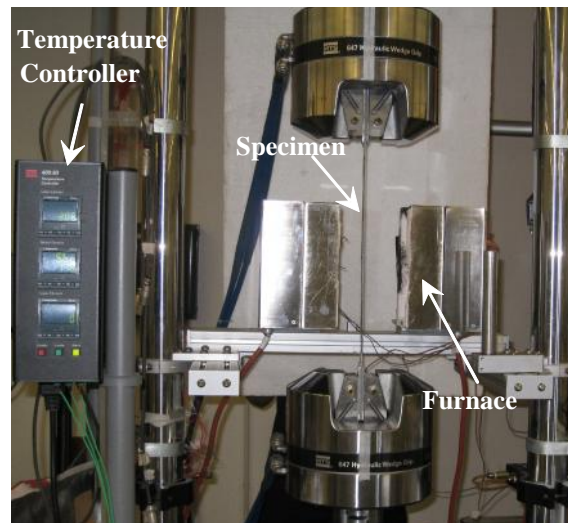


Figure 1. Test setup.

2.2 Test results

A detailed account of the test results are provided in Wang et al. [12] and a summary is provided herein. The results of Group G2 tests show that the ultimate strength and failure modes for the specimens were almost the same as compared to the corresponding specimens in Group G1. The epoxy was found to be affected by the elevated temperature regardless of exposure duration. It can therefore be concluded that the holding time of 5 minutes was sufficient to achieve representative results. The tensile stress-displacement curves though exhibited temperature dependent features as can be observed in Figure 2, namely, the ultimate strength deteriorated when exposed to elevated temperature. Figure 2 shows the stress-displacement relationship to be essentially linear from room temperature to temperatures as high as 520°C right up to rupture failure. In addition, for temperatures ranging from 625°C to the maximum temperature of 706°C, the stress-displacement relationships become non-linear at high stress levels as a result of fibre loss due to oxidation.

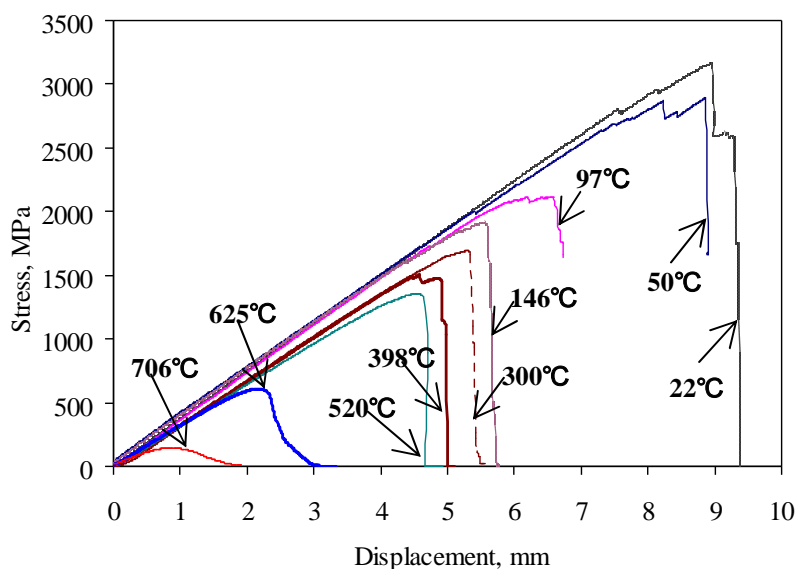


Figure 2. Stress-displacement relationship of G1 [12]

A brief description of all failure modes encountered in all tests is provided herein. Four different failure modes can be defined, based on the group G1 test specimens with increasing temperature, which are herein referred to as Modes I, II, III and IV. Each of the failure modes are defined in terms of the temperature ranges extracted directly from the information provided in Table 1.

Table 1. Temperature, ultimate stress and failure mode of tests at elevated temperatures [12]

Group	Specimen Identification ¹	Temperature T (°C)	Holding Time (min)	Ultimate Stress ² $f_{u,T}$ (MPa)	$\frac{f_{u,T}}{f_{u,normal}}$	Failure Mode ³
G1 (Temperature Series)	SS-22-0-1	22	0	3239.3	1.034	I
	SS-22-0-2	22	0	3169.8	1.011	I
	SS-22-0-3	22	0	3052.1	0.974	I
	SS-22-0-4	22	0	3072.5	0.980	I
	SS-50-5-1	50	5	2889.6	0.922	I
	SS-50-5-2	50	5	3110.7	0.993	I
	SS-100-5-1	98	5	2197.6	0.701	II
	SS-100-5-2	103	5	2137.0	0.682	II
	SS-100-5-3	97	5	2118.1	0.676	II
	SS-150-5-1	146	5	1916.8	0.612	II
	SS-150-5-1	155	5	1792.8	0.572	II
	SS-150-5-1	150	5	1944.0	0.620	II
	SS-200-5-1	211	5	1690.3	0.539	II
	SS-200-5-2	203	5	1720.7	0.549	II
	SS-200-5-3	181	5	1728.9	0.552	II
	SS-200-5-4	198	5	1731.1	0.552	II
	SS-300-5-1	308	5	1664.2	0.531	II
	SS-300-5-2	279	5	1704.4	0.544	II
	SS-300-5-3	300	5	1693.8	0.541	II
	SS-400-5-1	395	5	1501.9	0.479	III
	SS-400-5-2	398	5	1504.2	0.480	III
	SS-400-5-3	420	5	1489.4	0.475	III
	SS-500-5-1	520	5	1354.5	0.432	III
	SS-500-5-2	500	5	1340.8	0.428	III
SS-600-5-1	623	5	689.5	0.220	III	
SS-600-5-2	625	5	609.1	0.194	III	
SS-700-5-1	706	5	143.5	0.046	IV	
SS-700-5-2	698	5	223.2	0.071	IV	
G2 (Time Series)	SS-150-30-1	152	30	1858.0	0.593	II
	SS-150-30-2	180	30	1776.4	0.567	II
	SS-150-30-3	163	30	2002.6	0.639	II
G3 (Stress Series)	TS-1000-1	600	-	1061.0	0.339	III
	TS-1500-1	508	-	1500.0	0.479	II
	TS-2000-1	135	-	2000.0	0.638	I

¹ SS-50-5-1: SS = Steady State, 50 = target temperature of specimen at failure, 5 = holding time at target temperature, 1 = first specimen in sub-series.

TS-1000-1: TS = Transient State, 1000 = target stress of specimen, 1 = first specimen in sub-series

² For calculation of the ultimate stress, the measured width and thickness of the specimen were used to determine the cross-sectional area of the specimen [12].

³ Failure modes described in text.

Mode I

The temperature to cause Mode I failure was relatively low and ranged from 22°C to 50°C. The specimens primarily failed in a brittle fibre rupture fashion and the ruptured simultaneously at different positions along the length of the specimens. The failure modes do not appear to have been influenced by these temperatures.

Mode II

For specimens failing in a Mode II manner, the rupture position was always in the region of the furnace. This failure mode occurred between temperatures ranging from 97°C to 308°C. Such specimens experienced softening and gasification of the epoxy resin matrix followed by fibre rupture.

Mode III

For temperatures ranging from 395°C to 625°C, the specimens failed in a Mode III manner. For this failure mode, there was no epoxy left on the pultruded FRP plate inside the furnace because the epoxy had self-ignited at about 350°C.

Mode IV

Mode IV failing specimens fell within temperatures ranging from 698 up to 706°C. For these specimens, the epoxy was completely burned and about half of the carbon fibres had oxidised.

The failure temperature for each of the specimens in the G3 series tests was deemed to be reached when the tensile load was no longer sustained. The failure temperatures of the test specimens of Series G3 in the transient state are given in Table 1. The comparison between the steady state and transient state test results is also plotted in Figure 3. In this figure, the vertical axis represents the strength reduction ratio $f_{u,T}/f_{u,normal}$ and the horizontal axis represents the temperature ($f_{u,T}$ = ultimate stress at temperature $T^{\circ}\text{C}$, $f_{u,normal}$ = ultimate stress at normal room temperature 22°C). An abrupt drop of failure temperatures when the stress ratio ($f_{u,T}/f_{u,normal}$) was increased from 0.34 to 0.65 can be noted. In addition, it was also found that the transient state test results were slightly higher than those obtained from the steady state tests under a certain load level.

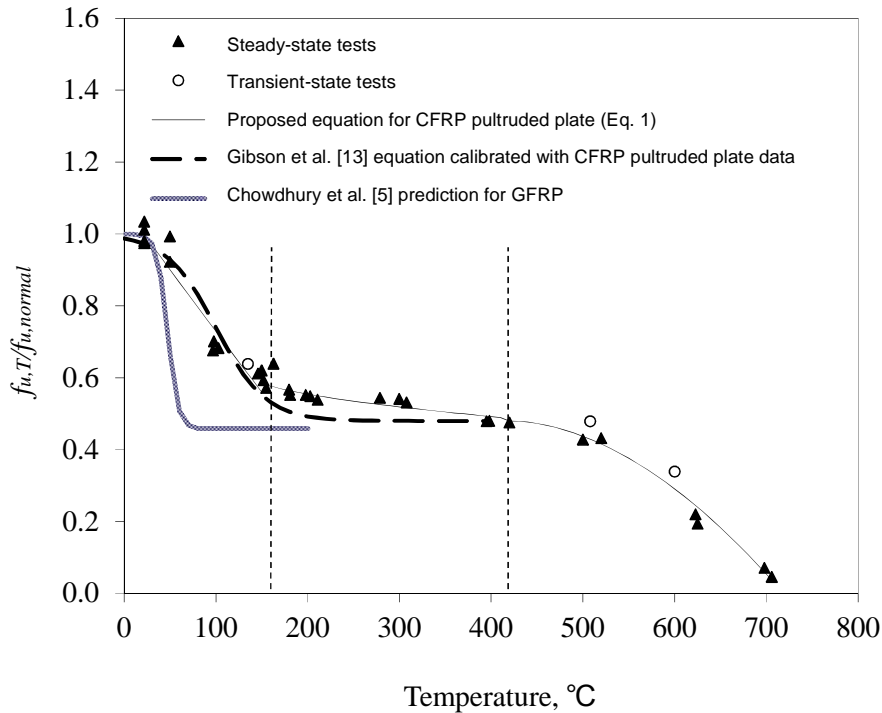


Figure 3. Ultimate plate strength: test results and predictions [12]

Figure 3 also shows that two large reductions of the failure strength of the test specimens occurred at temperature ranges of 22°C to 150°C and 450°C to 706°C. In between these temperature ranges there was a gradual reduction in strength while at 300°C the ultimate strength of the test specimens reduced to approximately 50% to that of the room temperature results. In addition, as the temperature rose to 706°C, the test specimens experienced a significant drop in strength compared with the room temperature tested specimens.

3. Proposed equation for ultimate strength and worked example

In recent years, researchers have been developing models to predict the elevated temperature behaviour of FRP materials formed from different fibres and manufacturing procedures. There have, however, been more experimental investigations by comparison to date. Of the few analytical models developed, Gibson et al. [13] for example proposed a model which was derived from composite laminate theory for elevated temperatures up to 200°C. Their model utilised a hyperbolic tangent function which predicted the temperature evolution through the thickness and the profile of the residual resin content, which in turn reflected the extent of thermal damage of the FRP. Afterwards, Chowdhury et al. [5] calibrated Gibson's [13] model with glass FRP (GFRP) coupon tests and FRP-to-FRP bond strength tests also for temperatures up to 200°C.

The model proposed by Chowdhury et al. [5] is plotted in Figure 3. It can be observed that the model provides a conservative lower bound due to the model being calibrated from tests on a different FRP material instead of pultruded CFRP plates as investigated in this study. Chowdhury et al.'s [5] results on GFRP coupons show degradation at a greater rate than the pultruded CFRP plate coupons presented herein. The original form of Chowdhury et al.'s [5] model (as defined in Gibson et al. [13]) is now re-calibrated with the pultruded CFRP plate data presented in this paper. The range of data extends up to 395°C which physically represents the complete vaporization of the epoxy. The model is, however, limited to temperatures up to about 400°C. A new modelling

approach is therefore required in order to describe the complete tested temperature range.

The newly proposed model is inspired from the modelling of metals subjected to high temperatures. More specifically, the stress-temperature relationship for the CFRP pultruded plates reported herein exhibited the same shape as elevated temperature tests on stainless steel and cold-formed steel materials conducted by Chen and Young [14, 15]. As a result, the stress-temperature model presented in Chen and Young [14, 15] and given in Eq. (1), is proposed to be used herein for CFRP plates at elevated temperatures.

$$\frac{f_{u,T}}{f_{u,normal}} = A - \frac{(T - B)^n}{C} \quad (1)$$

The coefficients A, B, C and n , which are calibrated with the results in Table 1, are presented in Table 2. Despite the small scatter in the data in the three zones (i.e. the R^2 of three zones are 0.90, 0.82 and 0.96, respectively), the model is robust and is capable of describing the entire temperature range. The model also forms a framework for future testing of composite materials at elevated temperatures and can readily be incorporated into design guidelines. Further details of the model are provided in Wang et al. [15].

Table 2. Coefficients of proposed ultimate strength equation. [12]

Temperature (°C)	Coefficients			
	A	B	C	n
22 T < 150	1.00	22	200	0.9
150 T < 420	0.59	150	490	0.7
420 T < 706	0.48	420	76000	1.8

The following worked example demonstrates application of Eq. 1.

Question:

Determine the ultimate strength ($f_{u,T}$) of a pultruded CFRP plate at 100, 400, 650°C. Given that the ultimate strength of the pultruded CFRP plate at room temperature ($f_{u,normal}$) is 3100 MPa.

Solution:

At temperature $T = 100^\circ\text{C}$, the coefficients of the proposed ultimate strength equation obtained from Table 2 are $A = 1.00$; $B = 22$; $C = 200$ and $n = 0.9$. Now, using Eq. 1 of the proposed model at elevated temperature, $\frac{f_{u,T}}{3100} = 1.00 - \frac{(100 - 22)^{0.9}}{200}$. Therefore, $f_{u,T} = 2318$ MPa at 100°C .

At temperature $T = 400^\circ\text{C}$, the coefficients of the proposed ultimate strength equation obtained from Table 2 are $A = 0.59$; $B = 150$; $C = 490$ and $n = 0.7$. Substitution of the coefficients into Eq. 1 yields $\frac{f_{u,T}}{3100} = 0.59 - \frac{(400 - 150)^{0.7}}{490}$. Therefore, $f_{u,T} = 1527$ MPa at 400°C .

At temperature $T = 650^\circ\text{C}$, the results of Table 2 produces $A = 0.48$; $B = 420$; $C = 76000$ and $n = 1.8$, and Eq. 1 yields $\frac{f_{u,T}}{3100} = 0.48 - \frac{(650 - 420)^{1.8}}{76000}$. Therefore, $f_{u,T} = 761$ MPa at 650°C .

Suitable factors of safety can facilitate the use of Eq. 1 in a design situation. Specification of such factors is outside the scope of this paper and is therefore identified as necessary future research.

4. Conclusions

This paper has reported a new model for predicting the ultimate load carrying capacity of CFRP pultruded plates subjected to temperatures ranging from room temperature to temperatures as high as 700°C. In order to calibrate the model, a series of tests has also been reported which consider both steady state and transient state test conditions. It should be noted that the results are specific to the type of resin and fibre as well as the fibre volume fraction of the plate tested although a suitable framework for future investigations has been established. In the steady state tests, the temperatures ranged from approximately 20 to 700°C, whereas in the transient state tests the stress ratios ranged from 0.34 to 0.64. The failure modes and ultimate strengths of the test have been discussed and the stress-displacement relationships have been plotted. Four different failure modes were identified and described, namely (i) rupture of the FRP plate (Mode I), (ii) partial loss of epoxy matrix followed by plate rupture (Mode II), (iii) complete loss of epoxy matrix (Mode III), and (iv) complete loss of epoxy matrix as well as considerable oxidation of the carbon fibres (Mode IV). At temperatures from around 200 to 300°C, the ultimate strength of the plates reduced to approximately 50% to that of room temperature strengths. In addition, when the temperature rose to around 700°C, the test specimens experienced a significant drop in strength compared to the room temperature strengths. Future testing should consider different fibres and epoxies as well as different methods of manufacture in order to calibrate the model over a much wider range of parameters. Finally, application of the model has been demonstrated in a worked example. The need to determine suitable factors of safety for application of the model in a design situation has been identified.

References

- [1] HOLLAWAY L.C. and TENG J.G. (2008). *Strengthening and Rehabilitation of Civil Infrastructures using Fibre-Reinforced Polymer (FRP) Composites*, Woodhead Publishing Limited, Cambridge, UK.
- [2] LEONE M., MATTHYS S. and AIELLO M.A. (2009). “Effect of elevated service temperature on bond between FRP EBR systems and concrete”, *Composites: Part B*, Vol. 40, pp. 85-93.
- [3] FOSTER S.K. and BISBY L.A. (2008). “Fire survivability of externally bonded FRP strengthening systems”, *Journal of Composites for Construction*, ASCE, Vol. 12, No. 5, pp. 553-561.
- [4] EEDSON R.T., BISBY L.A. and GREEN M.F. (2009). “Performance of FRP strengthening systems for concrete during exposure to elevated temperatures.” Proceedings (CD-Rom), *9th International Symposium on Fiber Reinforced Polymer Reinforcement for Concrete Structures (FRPRCS-9)*, July 13-15, 2009, Sydney, Australia.
- [5] CHOWDHURY E.U., EEDSON R., GREEN M.F., BISBY L.A. and BENICHOU N. (2009). “Mechanical characterization of fibre reinforced polymers materials at high temperature”, *Fire Technology*, Vol. 45, No. 4, pp. 1-18.
- [6] CAO S., WU Z. and WANG X. (2009). “Tensile properties of CFRP and hybrid FRP composites at elevated temperatures”, *Journal of Composite Materials*, Vol. 43, No. 4, pp. 315-330.
- [7] HAN L.H., WANG W.H. and YU H.X. (2010). “Experimental behaviour of reinforced concrete (RC) beam to concrete-filled steel tubular (CFST) column frames subjected to ISO-834 standard fire ”, *Engineering Structures*, Vol. 32, No. 10, pp. 3130-3144.
- [8] LIM L., BUCHANAN A.H. and MOSS P.J. (2004). “Numerical modelling of two-way reinforced concrete slabs in fire”, *Engineering Structures*, Vol. 26, No. 8, pp. 1081–1091.

- [9] LIM J.B.P. and YOUNG B. (2007). "Effects of elevated temperatures on bolted moment-connections between cold-formed steel members", *Engineering Structures*, Vol. 29, No. 10, pp. 2419-2427.
- [10] TO E.C.Y. and YOUNG B. (2008). "Performance of cold-formed stainless steel tubular columns at elevated temperatures", *Engineering Structures*, Vol. 30, No. 7, pp. 2012-2021.
- [11] ACI440.3R-04 (2004). *Guide Test Methods for Fiber-Reinforced Polymers (FRPs) for Reinforcing or Strengthening Concrete Structures*, American Concrete Institute, Farmington Hills, USA.
- [12] WANG K. YOUNG B. and SMITH S.T. (2011). "Mechanical properties of pultruded carbon fibre-reinforced polymer (CFRP) plates at elevated temperatures". *Engineering Structures*, Vol. 33, pp. 2154-2161.
- [13] GIBSON A.G., WU Y.S., EVANS J.T. and MOURITZ A.P. (2006). "Laminate theory analysis of composites under load in fire", *J Compos Mater* , Vol. 40, No. 7, pp. 639– 657.
- [14] CHEN J. and YOUNG B. (2006). "Stress–strain curves for stainless steel at elevated temperatures", *Engineering Structures*, Vol. 28, No. 2, pp. 229-239
- [15] CHEN J. and YOUNG B. (2007). "Experimental investigation of cold-formed steel material at elevated temperatures", *Thin-walled Structures*, Vol. 45, No. 1, pp. 96-110.